universität wien

MASTERARBEIT / MASTER'S THESIS

Titel der Masterarbeit / Title of the Master's Thesis

Effects of placebo and nocebo on resting-state functional connectivity

verfasst von / submitted by

Philipp Wagner, BSc

angestrebter akademischer Grad / in partial fulfilment of the requirements for the degree of

Master of Science (MSc)

Wien, 2019 / Vienna 2019

Studienkennzahl lt. Studienblatt / degree programme code as it appears on the student record sheet:	A 066 840
Studienrichtung lt. Studienblatt / degree programme as it appears on the student record sheet:	Masterstudium Psychologie UG2002
Betreut von / Supervisor:	Univ.-Prof. Mag. Dr. Claus Lamm
Mitbetreut von / Co-Supervisor:	Mag. Dr. Isabella Wagner, PhD

LIST OF CONTENTS

Abstract **4**

Abstract (deutsch) **5**

1.Introduction **7**

2. Material and Methods **11**

2.1. Participants 11

2.2. Study setup and experimental design 11

2.2.1.Behavioural session and pain calibration 12

2.2.2 fMRI sessions and experimental manipulation 12

2.2.3. Scanning procedure 13

2.3. MRI data acquisition 14

2.4. Data processing and statistical analysis 15

2.4.1. MRI data preprocessing 15

2.4.2. Group Independent Component Analysis (Group-ICA) 16

2.4.3. Within-network connectivity 19

2.4.4. Between-network connectivity 20

3. Results **21**

3.1. Expectation of Effectiveness of Medication 21

3.2. Within-network connectivity 21

3.3. Between-network connectivity across groups 23

3.4. Group differences in between-network connectivity 25

4. Discussion **27**

5. Conclusion **30**

References **31**

Abstract

Believed effectiveness in an inactive treatment can lead to positive or negative responses not attributive towards the treatment. This effect, depending on the direction, is known as the placebo or nocebo effect, respectively. Evidence shows that both phenomena are repeatedly found in a brain areas involved in pain perception. Resting-state functional connectivity, the measurement of spontaneous activity can identify a set of separated brain regions which show highly correlated neuronal activity, known as resting-state networks (RSNs). The set of brain regions involved in placebo analgesia and nocebo hyperalgesia show spatial resemblance to some of the RSNs. Yet, whether and how placebo/nocebo manipulation influence resting-state connectivity is still poorly understood. To investigate these influences, we analysed the resting-state functional magnetic resonance imaging data from 35 participants after undergoing placebo/nocebo manipulation and compared it to a control condition. Within the nocebo group, we found increased connectivity of the medial prefrontal cortex in a network resembling the so-called *default-mode network*. Further, higher connectivity between-networks comprising brain regions of the brain stem, amygdala, insular and anterior cingulate cortex was found. This resembles a network typically associated with descending pathway for pain modulation and activity within this network is repeatedly found during the placebo effect. Thus, these findings support previous evidence of cognitive modulation during the placebo and nocebo effect.

.

Abstract (deutsch)

Die geglaubte Wirksamkeit an eine inaktiven Behandlung kann zu positiven oder negativen Behandlungsergebnissen führen, welche der Behandlung nicht zugesprochen werden kann. Dieser Effekt wird, je nach Richtung, als Placebo- bzw. Nocebo-Effekt bezeichnet. Es konnte vielfach gezeigt werden, dass beide Effekte wiederholt Aktivität in einem System von Gehirnregionen hervorrufen, welches an der Schmerzwahrnehmung beteiligt ist.

Funktionelle Konnektivität im Ruhezustand, bei dem die spontane Konnektivität im Gehirn gemessen wird, kann eine Reihe räumlich getrennter Hirnregionen identifizieren, welche eine stark korrelierte neuronale Aktivität aufweisen. Diese werden auch als Ruhezustandsnetzwerke (RSNs) bezeichnet. Dabei gibt es Ähnlichkeiten zwischen den involvierten Gehirnarealen einiger RSNs und den Gehirnarealen, die beim Placebo- und Nocebo-Effekt involviert sind. Jedoch ob und wie der Placebo- und Nocebo-Effekt die funktionelle Konnektivität im Ruhezustand beeinflussen, ist noch unausreichend verstanden. Wir haben daher diese Einflüsse untersucht, indem wir die funktionellen Magnetresonanztomographie-Daten von 35 ProbandInnen im Ruhezustand untersucht haben. ProbandInnen unterliefen einer Placebo- oder Nocebo-Manipulation und wurden mit einer Kontroll Messung verglichen.

Die Ergebnisse zeigten eine stärkere Aktivierung des medialen präfrontalen Cortex in der Nocebo-Gruppe für ein RSN, das dem sogenannten *Default-mode-network* entspricht. Des Weiteren wurde eine höhere Konnektivität zwischen RSNs in der Placebogruppe gefunden, die den Hirnstamm, Amygdala, insularen und anterioren Kortex umfassen. Dies entspricht einem Netzwerk, welches mit dem absteigenden Signalwegs der Schmerzunterdrückung assoziiert wird und Involviertheit im Placebo-Effekt aufweist. Diese Funde stützen frühere Ergebnisse kognitive Modulation des Placebo- und Nocebo-Effekts und zeigen deren Auswirkungen auf RSNs.

1.Introduction

The International Association for the Study of Pain defines pain as „an unpleasant sensory and emotional experience associated with actual or potential tissue damage, or described in terms of such damage“(Merksey & Bogduk, 1994). However, pain is a complex, multidimensional subjective sensation and often shows a nonlinear relationship between perceived pain and nociceptive input (Wiech, Ploner & Tracey, 2008). The nonlinear relationship can be demonstrated by simply shifting the focus of attention towards or away from the nociceptive stimuli and thus modulating perceived intensity (Terkelsen et al., 2004), but other factors like memories, genetics or emotions can also shape experienced pain (Tracey & Mantyh, 2007).

Neurophysiological and neuroimaging studies have shown that nociceptive stimuli activate responses in a wide array of brain areas, including parietal, frontal and somatosensory areas, as well as insular and cingulate areas (Legrain, Iannetti, Plaghki & Mouraux, 2011). This network, originally named “neuromatrix” (Melzack, 1990) but later changed into “pain matrix” (Tracey, & Johns, 2010; Mouraux, Diukova,Lee, Wise & Iannetti, 2011), is now a candidate biomarker for pain and drug discovery (Salomons, Iannetti, Liang & Wood, 2016). However, there is still no consensus whether a unique pattern for pain exists, but hopefully through the inclusion of newer techniques like machine-learning algorithms (see Wager et al., 2013) and multimodal approaches (Lee et al., 2019), we get a broader understanding of the involved processes (see also Iannetti, Salomons, Moayedi, Mouraux & Karen, 2013 for a critic on the pain matrix)

Of special interest for this master’s thesis are the cognitive processes involved in pain perception, which can lead to the so called placebo or nocebo effect. The placebo (Latin “I shall please”) and nocebo (Latin “I shall harm”) effect refer to the positive and negative cognitive modulation of behaviours and outcomes related to an inactive treatment, respectively (Colloca & Grillon, 2014). Conscious expectation and unconscious classical conditioning, reward-learning, observational and social learning, modulation of anxiety, desire, motivation, memory and prior experience, somatic focus, personality traits and genetics work as facilitators of the placebo or nocebo effect (Testa & Rossettini, 2016). These effects can directly influence clinical pharmacological trials and medical research (Zaccara, Giovannelli & Schmidt, 2015) and methods are needed

to reduce placebo and nocebo as confounding influences (Egorova et al., 2015; Colloca, Schenk, Nathan, Robinson & Grillon, 2019). But it also provides a way to investigate how brain systems process contextual information (Wager & Atlas, 2015) and potentially tailor patient-clinician communication to reduce nocebo induced hyperalgesia and increase placebo induced analgesia in these settings (Colloca, 2017).

On a biochemical level, placebo analgesia is most often associated to work through endogenous opioids, which was first demonstrated by Levine, Gordon and Fields (1979) by administering naloxone, an opioid antagonist, which canceled out the placebo effect. But endogenous dopamine, oxytocin, cannabinoids, serotonin and vasopressin are also involved in placebo analgesia, while nocebo hyperalgesia on the contrary works through cholecystokinin and cyclooxygenase-prostaglandins, or inhibiting dopamine and opioid expression (Testa & Rossettini, 2016; Benedetti, 2014; Benedetti, Mayberg, Wager, Stohler & Zubieta, 2005).

Studies using functional magnetic resonance imaging (fMRI) to study the placebo effect typically report activation of the rostral anterior cingulate cortex (rACC) and the periaqueductal grey (PAG). Together with the rostroventral medulla (RVM), these areas are referred to the descending pathway of pain modulation(Eippert et al., 2009), inhibiting nociceptive processing at the level of the spinal cord.

Increased activity following placebo analgesia is also typically observed in the lateral prefrontal cortex (lPFC), thalamus, insula (INS), amygdala, nucleus accumbens (NAc), primary and the secondary somatosensory cortex (S1 & S2; Amanzio, Benedetti, Porro, Palermo & Cauda, 2013; Atlas & Wager, 2014; Atlas & Wagner, 2015).

Studies focusing on the nocebo effect also report brain regions associated with the descending pathway for pain modulation (Tracey, 2010). The different modulation of pain is thought to be partly attributed by cognitive reappraisal stemming from the orbitofrontal cortex (OFC), ventromedial prefrontal cortex (vmPFC) and right lPFC. This is theorised as a fear-anxiety network, exerting nocebo hyperalgesia mainly through an inhibition by the rACC (Wager, 2005). This network further comprises brain regions of the dorsal ACC, INS, superior parietal lobule and parietal operculum, as well as the hippocampus (Kong et al., 2008).

Despite the amount of research in the field of placebo and nocebo, still the question remains whether placebo and nocebo are different cognitive constructs with different

brain networks involved (Kong et al., 2008; Freeman et al., 2015), or, with the words of Petrovic (2008) are “two sides of the same coin” and can be represented as a continuum (Pollo & Benedetti, 2011).

Resting-state functional connectivity, the study of low-frequency fluctuations using the oxygen level dependent contrast of participants at rest, can be used to identify functionally relevant resting-state networks (RSNs, Luca, Beckmann, Stefano, Matthews & Smith, 2006). Functional connectivity is often described as the temporal dependency of neuronal activation patterns of anatomically separated brain regions (van den Heuvel & Pol, 2010). RSNs have been described in many studies, with slight variations between the classifications (see Damoiseaux et al., 2006 or Mantini, Perrucci, Gratta, Romani & Corbetta, 2007). The most commonly known RSN, the so called default-mode network (DMN), comprises a set of brain regions that are typically deactivated during performance, such as the medial prefrontal cortex (mPFC), medial temporal lobes (mTLs), and posterior cingulate cortex (pCC, Greicius, Supekar, Menon & Dougherty, 2008). Other RSNs reflect connectivity patterns that are similarly found during task-related measures, such as functions like executive functioning, auditory processing, motor function, visual processing and memory (Damoiseaux et al., 2006). Further, the RSNs called salience network (SN), sensorimotor network (SMN), frontoparietal network (FPN) and executive control network (ECN; Seeley et al., 2007) involve regions that are also activated during placebo analgesia and nocebo hyperalgesia. The behavioural importance of RSNs was further highlighted by using resting-state fMRI to predict the responsiveness of subjects towards the placebo effect. Kong and colleagues (2013) could show that functional connectivity between the FPN and the rACC/mPFC was positively associated with placebo effectiveness. Sikora and colleagues (2016) found increased connectivity between the SN and rACC for patients with major depressive disorder who showed greater symptom reduction after placebo treatment (Sikora et al., 2016). Hashimi and colleagues (2012) found similar patterns for people with chronic back pain and responsiveness towards the placebo effect, where higher connectivity within the left mPFC and bilateral INS accurately predicted placebo analgesia. Yu and colleagues (2014) found a negative association of the ventral striatum and placebo responsiveness, further supporting previous evidence that reward

networks are an important factor within placebo analgesia, theorised to work through expectancy of pain relieve (Atlas et al., 2010).
Influences of the nocebo effect on resting-state connectivity were found with increased connectivity between the operculum and the superior temporal gyrus, which was correlated with higher pain ratings for heat stimuli in a following task (Ellerbrock et al., 2015). Van de Sand and colleagues (2018) could find a positive coupling between the insula and periaqueductal grey within a nocebo group, which was associated with higher itch-sensations (van de Sand, Menz, Sprenger & Büchel, 2018).

Therefore, we investigated the effects of nocebo and placebo on resting-state networks in healthy participants in a mixed design, with nocebo and placebo groups and within-participant control sessions. 44 participants were randomly assigned to a placebo or nocebo group and underwent fMRI during two different scanning sessions (of which one was the experimental session and the other the control session). The collected resting-state data was then compared between groups and between sessions to measure for within-network and between-network connectivity differences. Given the divergence of reported brain areas involved with the placebo and nocebo effect between studies and these influences on RSNs, we chose an exploratory and predominantly data-driven analysis using independent component analysis.
We expected to find decreased within-network connectivity for the SMN and increased within-network connectivity for the SN and FPN for the within-placebo group comparison, based on commonly reported brain areas associated with these RSNs (Atlas & Wager, 2014).
We further expected find decreased within-network connectivity for the ECN and increased within-network connectivity for the DMN and the SN for the within-nocebo group comparison (Rief, Bingel, Schedlowski & Enck, 2011; Freeman et al., 2015).
For between-network connectivity between the placebo and nocebo group, we expected to find different patterns mainly between the FPN, ECN, SN and SMN, based on previous studies investigating placebo- or nocebo-related connectivity changes (Kong et al., 2013; Sikora et al., 2016; van de Sand et al., 2018; Ellerbrock et al., 2015).

2. Material and Methods

2.1. Participants

For this study, 80 people were recruited of which 44 were included in this analysis due to limitations of server storage at the time of data collection (35 females, mean age = 23 years, age range = 18-32 years). Participants were randomly assigned to a placebo (N=21, 15 females, mean age = 23 years, age range = 19-32) or nocebo group (N=23, 18 females, mean age = 21 years, age range = 18-29 years). Exclusion criteria were alcohol and drug abuse as well as psychological or neurological disorders. All participants were healthy, right-handed, had normal or corrected-to-normal vision and gave written informed consent prior to participation. The study was reviewed and approved by the ethics committee of the Medical University of Vienna.

2.2. Study setup and experimental design

The study took place at three different sessions, with the first session (behavioural session) at the behavioural laboratory to conduct a pain calibration for the later experiments and get participants acquainted with the study design. Within the following two sessions (fMRI sessions), each participant took part in an experimental session (placebo or nocebo) and a control session. The assignment to the experimental group was randomised and the order of the experimental and control sessions were counterbalanced across participants. The fMRI sessions took place one week apart.

2.2.1.Behavioural session and pain calibration

During the pain calibration in session one, short-lasting electrical stimuli (duration = 500 ms) were delivered using a Digitimer DS5 Isolated Bipolar Constant Current Stimulator (Digitimer Clinical and Biomedical Research Instruments) via a concentric surface electrode with 7 mm diameter and a platinum pin attached to the back of the left hand (based on study design from Rütgen et al., 2015). Using a staircase procedure, participants had to rate stimuli with increasing intensity on an eight-point scale from 0 (”not painful”) to 8 (“extremely painful”; the extremely painful stimuli had to bearable without any pain induced movements as participants were told, to minimize movements during the scanning sessions). The pain calibration took on average around 15-30 min

and the determined pain threshold was later used during the fMRI sessions. Additionally, physiological measures like blood pressure, saliva samples and heart rate were collected.

2.2.2 fMRI sessions and experimental manipulation

During the fMRI sessions, participants arrived with a confederate from the study team of whom participants believed to be another participant. The general instructions for the experiment were given to them together, but participant and confederate were separated afterwards into different rooms with the explanation that while the participant would get prepared for the fMRI scanner, the confederate would perform another task. After the confederate left, another pain calibration was conducted to ensure that the pain threshold from the behavioural session was unchanged. Then, for the experimental manipulation, a medical doctor (a member of the experimental team) introduced himself to the participant. A lactose pill was administered and the participant was informed that it is not the goal of the study to analyse the effectiveness of the medication, as it is already established and commercially available. Further, depending on the experimental condition (nocebo, placebo or control), they were told that the medication would lead to an increase, decrease or change (without suggested direction) in pain perception, respectively. After the pill administration, participants rated their expected belief of the effectiveness of the medication on a Visual Analogue Scale (VAS; from 0 = “not effective” to 10 = “very effective”). A 15-minute break followed, allegedly so that the medication could take effect. To further amplify the effect from the verbal suggestion, participants underwent a commonly used condition procedure (see also Rütgen et al., 2015). Specifically, participants received a series of electrical stimuli that they previously rated as medium painful (the intensity they rated with 4 or 5 on the VAS). Within the placebo group, they were informed that they previously rated these stimuli as very painful (7 and 8 from VAS). For the nocebo group, participants also received medium painful stimuli (4 and 5 from VAS), but were led to believe that they had previously rated these stimuli as not painful (1 and 2 from VAS). Therefore, the conditioning procedure lead to a mismatch of believed and actual pain intensity. For the control group, conveyed information about the administered stimuli matched the actual intensity. After the conditioning procedure, participants again rated their expected belief of the effectiveness of the medication.

Participants knew that the confederate did not receive any medication and related questions about the medication were postponed to the end of the study, where participants were debriefed.

2.2.3. Scanning procedure

After the preparation and the experimental manipulation, participants went into the scanner room and were checked if the electrodes still delivered shocks as previous rated before the fMRI study began. Each session began with an eight minute resting-state measurement, followed by two tasks and a structural scan. This thesis only focuses on the resting-state connectivity, but the two tasks consisted of an empathy for pain task (see Lamm, Decety & Singer, 2011) and a reward-learning task (see Lockwood et al., 2016).

During the resting-state period, participants were instructed to relax and don't think of anything in particular. A fixation cross was presented, which randomly changed colour 3 times during the resting-state period. Each time the cross changed the colour, subjects had to press a button on a button box within their right hand to indicate that they are still awake.

2.3. MRI data acquisition

MRI data were acquired using a Siemens Magnetom Skyra 3 Tesla scanner equipped with a 32-channel head coil. 408 T_2*- weighted BOLD images were obtained during the resting-state period, using a multiband-accelerated echo planar imaging (EPI) sequence. Parameters were as follows: echo time (TE)/repetition time (TR) = 33/2180 ms, flip angle 90°, field of view (FOV), 224 x 224 mm; matrix, 74 x 74; 34 ascending axial slices; 21% slice gap; voxel size, 3 mm. Structural scans were acquired using a magnetization-prepared rapid gradient echo (MP-RAGE) sequence with the following parameters: TR, 2300 ms; TE, 3.03 ms; flip angle, 8°; FOV, 256 x 256 mm; voxel size, 1 mm isotropic.

2.4. Data processing and statistical analysis

2.4.1. MRI data preprocessing

All resting-state data were analysed using the Functional Magnetic Resonance Imaging of the Brain (FMRIB) Software Library (FSL, v5.0.1; https://fsl.fmrib.ox.ac.uk/fsl/fslwiki/; Smith et al., 2004) and Matlab (MATLAB 2019a, The MathWorks, Inc., Natick, Massachusetts, United States). First, the structural scans were processesed using *fsl_anat*, including reorienting images to the Montreal Neurological Institute (MNI) standard space (using *fslreorient2std*) and correcting for spatial intensity variations (also known as bias field or RF inhomogeneities), using FMRIB's Automated Segmentation Tool (*FAST*, https://fsl.fmrib.ox.ac.uk/fsl/fslwiki/FAST; Zhang, Brady & Smith, 2001). Further, images were brain-extracted (*BET*, https://fsl.fmrib.ox.ac.uk/fsl/fslwiki/BET; Jenkinson, Pechaud & Smith, 2005) and registered into standard space (using *FNIRT* and *FLIRT,* https://fsl.fmrib.ox.ac.uk/fsl/fslwiki/FLIRT; https://fsl.fmrib.ox.ac.uk/fsl/fslwiki/FNIRT). The functional images were preprocessed using *FEAT*, including motion correction (*MCFLIRT*, https://fsl.fmrib.ox.ac.uk/fsl/fslwiki/MCFLIRT; Jenkinson, Bannister, Brady & Smith, 2002), spatial smoothing using a Gaussian kernel (5 mm full-width at half maximum) and alignment of images to the bias-corrected, brain extracted structural image (*FLIRT*, https://fsl.fmrib.ox.ac.uk/fsl/fslwiki/FLIRT; Jenkinson & Smith, 2001) using boundary-based registration. After a visual inspection of the *FEAT* results, some registered images showed insufficient realignment.

As noted by Jenkinson (2001), Echo Planar Imaging images can suffer from geometric distortions, which originate from intrinsic magnetic field inhomogeneities near bone/tissue and air/tissue boundaries. Therefore, field maps were generated by using the phase images, brain extracted magnitude images and the difference of Echo Times using the *fsl_prepare_fieldmap* tool. The *FEAT* analysis was then re-run with the inclusion of the B0 fieldmaps, which resulted in overall smoother images. Still, nine people had to be excluded due to spatial distortions (e.g., with horns or dents in the images after image processing). This yielded in a reduced set of participants for the nocebo (N = 17) and placebo group (N = 18). Independent component analysis (ICA) was further applied to automatically detect and remove participant-specific motion-related artifacts (ICA-based strategy for Automatic Removal Of Motion Artifacts, *ICA-*

AROMA; Pruim et al., 2015a, 2015b). To circumvent problems with group normalisation, registration parameters were applied to the functional data (using *applywarp*).

2.4.2. Group Independent Component Analysis (Group-ICA)

For the group-ICA analysis, the procedure pipeline from Wagner et al. (2019) was followed. First, a high pass filter was used with a cut off at 0.01 Hz to remove low-frequency drifts, which can be caused by physiological or scanner related noise (Smith et al., 1999). Data from all participants were then concatenated into a time x voxel x participant matrix to yield a fourth-dimensional image which was then submitted to the Fsl tool *Melodic* (https://fsl.fmrib.ox.ac.uk/fsl/fslwiki/MELODIC; Beckmann and Smith, 2004) to calculate independent spatiotemporal components. Instead of using the automatic component estimation option from *Melodic,* 30 independent components (ICs) were identified, as it was shown by Aboud-Elseoud and colleagues (2009) that this yields the most common resting-state networks.

For evaluation, a manual and an automatic template-matching procedure was applied. For the manual inspection, the resting-state networks reported by Beckmann and colleagues (2005) were used as a comparison. 11 of the 30 ICs could be identified this way (and classified into one of the reported resting-state networks: (1) medial visual cortical network, (2) lateral visual cortical network, (3) auditory network, (4) sensory-motor network, (5) default-mode network, (6) executive control network, (7) left-, and (8) right dorsal visual networks, Beckmann et al., 2005)

Of the remaining 19 ICs, three were classified as noise (white matter) and 16 were ambiguous, as they couldn't be attributed exclusively to one of the RSNs. Therefore, the next step included automatic correlation to reference network templates (Smith et al., 2009; Yeo et al., 2011) using the Fsl tool *fslcc* (templates were downloaded from: https://www.fmrib.ox.ac.uk/datasets/brainmap+rsns/ ; https://surfer.nmr.mgh.harvard.edu/fswiki/CorticalParcellation_Yeo2011). Using the correlations from the two templates, the remaining ICs were further classified, which resulted in a final set of 27 ICs for all following analysis (Fig 1).

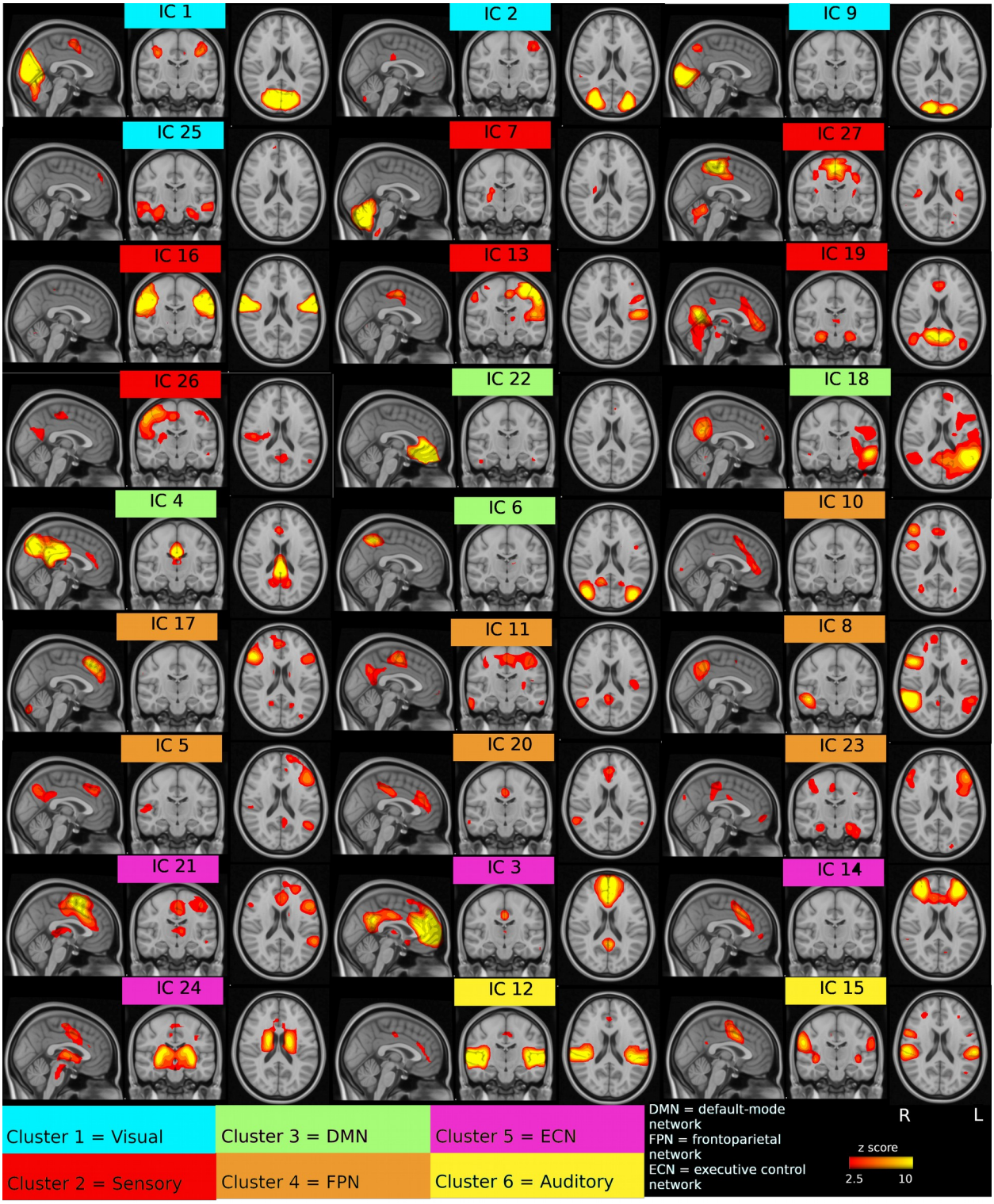

Fig. 1. Group-ICA results from all participants (N = 35) yielded 27 independent components (ICs) which were used for all further analysis. Based on their spatial similarity with common RSNs assessed through manual inspection and template comparison, six different clusters were identified: visual (blue), sensorymotor (red), default mode network (green), frontoparietal (orange), executive control (purple) and auditory (yellow). ICs are shown according to neurological convention: R, right; L, left.

2.4.3. Within-network connectivity

To determine differences within the group resting-state networks, the dual regression procedure from Beckmann, Mackay, Filippini & Smith (2009) was applied. This was done by generating subject-specific spatial maps and the associated time series from the group-average spatial maps generated by ICA-*Melodic* (2.4.2.), using FSL's *dual regression* (https://fsl.fmrib.ox.ac.uk/fsl/fslwiki/DualRegression; see also Nickerson et al., 2017).

This included two steps. First, to obtain a set of subject-specific time series, the group-average spatial maps were regressed into each subject's 4D space-time dataset. Further, those time series were regressed into the same 4D dataset, resulting in subject-specific spatial maps, one per group-level spatial map (Beckmann et al., 2009). Next, using Matlab, the subject-specific spatial maps were concatenated temporally to form group specific maps in order to identify large-scale patterns between the different experimental groups. Specifically, the subject-specific spatial maps from the different groups were concatenated and the following contrasts created to test for possible differences:

(1) Within-group differences for placebo and nocebo group respectively (placebo vs control & nocebo vs control). (2) Comparison of experimental groups (placebo vs nocebo) with and without control conditions. (3) Comparison of control sessions between groups ($control_{placebo}$ vs $control_{nocebo}$). (4) Order effects within-groups, to check whether order of control session or experimental session leads to differences.

For inference, FSL's tool *randomise* (https://fsl.fmrib.ox.ac.uk/fsl/fslwiki/Randomise) was used, a nonparametric permutation method using the standard 5000 permutations between each contrast (Winkler, Ridgway, Webster, Smith & Nichols, 2014). *Randomise* allows modelling using a standard general linear model design, where the output was based on a Threshold-Free Cluster Enhancement (TFCE) method, which enhances cluster-like structures while the image remains voxelwise (Smith & Nichols, 2009). Since *randomise* only corrects for multiple comparisons for each RSN of its own, significant thresholding was further bonferroni corrected for the 27 included networks, therefore $p < 0.000925$ (0.05 / (27*2)). For reporting clusters, both fsl tools *atlasquery* (https://fsl.fmrib.ox.ac.uk/fsl/fslwiki/Atlasquery) and *cluster* (https://fsl.fmrib.ox.ac.uk/fsl/fslwiki/Cluster#reporting) were used to identify cluster sizes,

peak cluster coordinates and using the atlases Harvard-Oxford cortical and subcortical structural atlas to label regions within the clusters.

2.4.4. Between-network connectivity

To further test for between-network connectivity across participants, the FSL Nets tool (Smith et al., 2013) was implemented in Matlab (http://fsl.fmrib.ox.ac.uk/fsl/fslwiki/FSLNets). Whole brain connectivity matrices were created from the individual network time series (Palacio et al., 2017) by using the already obtained individual network time series from dual regression (see 2.4.3.). Specifically, for each participant a 27×27 correlation matrix of all ICs was created, where each element represents the correlation strength (i.e., edge) between two nodes (Wagner et al., 2019).

Following the recommended steps from the provided matlab script, full and partial correlation coefficients were calculated. Afterwards, participant-specific network matrices were reshaped into a single row and combined into a participant × edges network matrix to generate the functional connectome of the whole group (mean network matrix, placebo and nocebo, Fig. 2). To group similar nodes, the full correlations from the mean network matrix were used to rearrange the 27 nodes into groups (using hierarchical clustering), based on their spatiotemporal characteristics (Fig. 3).

To test group differences for between-network connectivity, each network matrix edge (i.e., connection between two nodes) was tested separately, using a two-sample t-test with a general linear model design implemented in *randomise*, generating 5000 permutations.

3. Results

3.1. Expectation of Effectiveness of Medication

First, the effectiveness rating during the experimental manipulation at the preparation during the fMRI session was analysed (see 2.2.2.). Therefore, the rating on the VAS scale from pre-manipulation was compared to post-manipulation for the placebo and nocebo group with a paired-sample t-test. Effectiveness ratings were significantly different for the placebo pre rating (mean ± standard error of the mean, SEM: 4.73 ±

0.53) compared to post rating (6.48 ± 0.66, t(16) = -3.71, p = 0.002, [95% CI, -2.77, -0.75]), as well as for the nocebo pre (4.7 ± 0.65) compared to post rating (8.15 ± 0.64, t(16) = -5.3, p < 0.001, [95% CI, -4.83, -2.05]), showing that for both groups, the experimental manipulation lead to an increased believe in the effectiveness.

3.2. Within-network connectivity

Next, we turned to functional connectivity within the different RSNs. We expected to find different within-network connectivity patterns for the groups as stated in the introduction. Considering all possible contrasts (see 2.4.3.), only one significant result was found while correcting for multiple comparisons for the within-network connectivity analysis. This was the comparison of the nocebo and $control_{nocebo}$ vs placebo and $control_{placebo}$, where within the IC 22, which was classified as resembling the DMN, more connectivity of the frontal medial cortex in the nocebo compared to the placebo group (Table 1) was found. IC 22 comprised the anterior cingulate cortex, medial & lateral frontal cortices and the inferior temporal lobe. Additionally, within the same contrast there was also higher connectivity around the central sulcus, which was labeled as the postcentral and precentral gyrus, but that finding did not reach significance. This pattern of connectivity, although not passing significance when corrected for multiple comparison, was also found when contrasting the experimental conditions. Again, when comparing the nocebo and placebo groups, there was higher connectivity within the nocebo compared to the placebo group in the IC22, namely in areas labeled as precentral and postcentral gyrus, as well as frontal regions (frontal orbital cortex, frontal medial cortex and frontal pole, Table 2). Also, a comparison of the control conditions showed higher connectivity in prefrontal areas in the $control_{nocebo}$ group for IC22. Analysing order effects showed only a non-significant result in the placebo group. If people were in the experimental placebo session at session 1, there was more connectivity of the central gyrus, labeled either belonging to the precentral or postcentral gyrus in IC22.

In total, only the group comparison including control session passed significance, with higher involvement of the frontal medial cortex in the DMN within the nocebo group.

Table 1, showing the results of *randomise*, comparing nocebo and placebo group (including control sessions in both groups) for voxels with p < 0.000925 (bonferroni-corrected for multiple comparisons).
Reported are the MNI coordinates of peak voxel activation, maximum p-value and size of cluster.
Brain regions are reported as probability of peak voxel location belonging to the labeled region. Used atlases are Harvard-Oxford cortical and subcortical structural atlases. IC, independent component.

ICs, contrast and brain regions		MNI coordinates				cluster size
		x	y	z	p-value	(2mm³)
IC 22	Nocebo & Control-Nocebo > Placebo & Control-Placebo (N=70)					
	91.4 % Right Cerebral Cortex 84.0 % Frontal Medial Cortex 6.0 % Subcallosal Cortex	2	34	-20	.0008	15

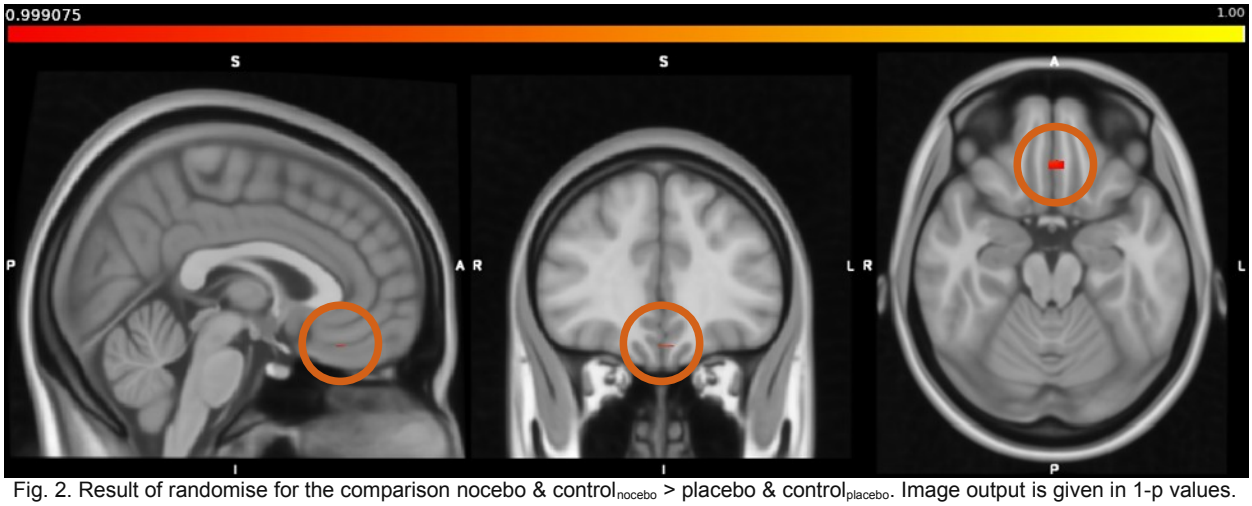

Fig. 2. Result of randomise for the comparison nocebo & control$_{nocebo}$ > placebo & control$_{placebo}$. Image output is given in 1-p values. Threshold is set to correct for multiple comparisons to only show voxels with p < 0.000925. For display purpose results are shown within coloured circle. Orientation labels: P = posterior; A = anterior; S = superior; I = inferior; R = right; L = left.

Table 2, showing the results of *randomise* for the different contrasts for voxels with $p < 0.05$.
Reported are the MNI coordinates of peak voxel activation, maximum p-value and size of cluster.
Brain regions are reported as probability of peak voxel location belonging to labeled region. Used atlases are Harvard-Oxford cortical and subcortical structural atlases. IC, independent component.

ICs, contrast and brain regions	MNI coordinates				cluster size
	x	y	z	p-value	(2mm³)
IC 22 Nocebo & $Control_{Nocebo}$ > Placebo & $Control_{Placebo}$ (N=70)					
91.4 % Right Cerebral Cortex 84.0 % Frontal Medial Cortex 6.0 % Subcallosal Cortex	2	34	-20	.0008	1442
39.0 % Precentral Gyrus 30.0 % Postcentral Gyrus	46	-10	32	.0.23	246
IC 22 Nocebo > Placebo (N=35)					
63.8 % Right Cerebral Cortex 29.0 % Inferior Frontal Gyrus, pars triangular 24.0 % Frontal Pole 3.0 % Middle Frontal Gyrus	46	34	12	.008	134
52.2 % Left Cerebral Cortex 40.0 % Precentral Gyrus 7.0 % Postcentral Gyrus	-38	-14	44	.029	85
IC 22 $Control_{Nocebo}$ > $Control_{Placebo}$ (N=35)					
51.0 % Frontal Orbital Cortex 10.0 % Frontal Medial Cortex 7.0 % Frontal Pole	-10	30	-24	.012	105
Order effects, Session 1 Placebo, session 2 $Control_{Placebo}$ (N=11)					
IC 22 $Control_{Placebo}$ > Placebo					
27.0 % Postcentral Gyrus 23.0 % Precentral Gyrus	-42	-14	32	.043	3

3.3. Between-network connectivity across groups

27 RSNs were identified, which were used as nodes in the network modeling. First, a mean network connectivity matrix was calculated and networks were grouped using hierarchical clustering (Fig. 3 and 4).

Four clusters were obtained from the hierarchical clustering. The first cluster (seen as purple, top left) consisted of two groups, where the left-most contains visual networks (IC 1, 9, 2) but was connected with two RSN that were classified as belonging to the

DMN (IC 4, 6). The second cluster (light blue) consisted of two FPNs (IC 17, 20), connected with ECN (IC 14) and visual (IC 8) networks. The third cluster (green) consisted of three groups. The first group on the left comprised FPNs (IC 10, 23) and SMN (IC 13), whereas the right group consisted of two auditory (IC 12, 15) networks, which are interconnected with SMN (IC 16, 26) and ECN (IC 21) networks. The last cluster comprised the ECN (IC 3, 24), FPN (IC 5, 11), and the SMN (IC 7, 19, 27) networks. In summary, the hierarchical clustering showed four different groups, where the first two groups were grouped mostly with similar networks and cluster three and four showed different RSNs grouped together, consisting of FPNs, ECNs and SMNs.

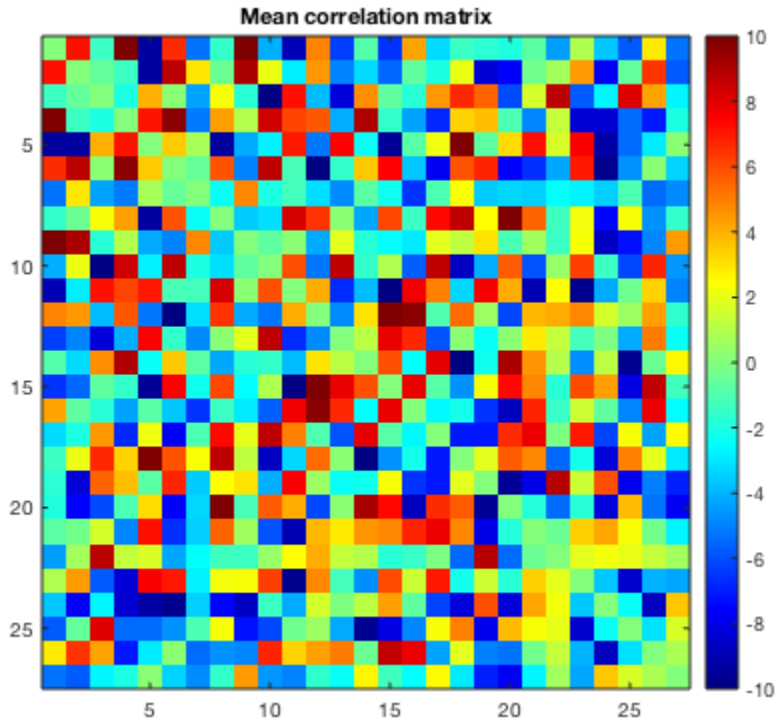

Fig. 3 The mean connectivity matrix across all participants (N = 35) with 27 nodes, which were defined during ICA. Each element represents the functional connectivity strength between two nodes (i.e., independent components from group-ICA). Blue represents negative and red positive correlation at the specific edge (i.e., connection between nodes).

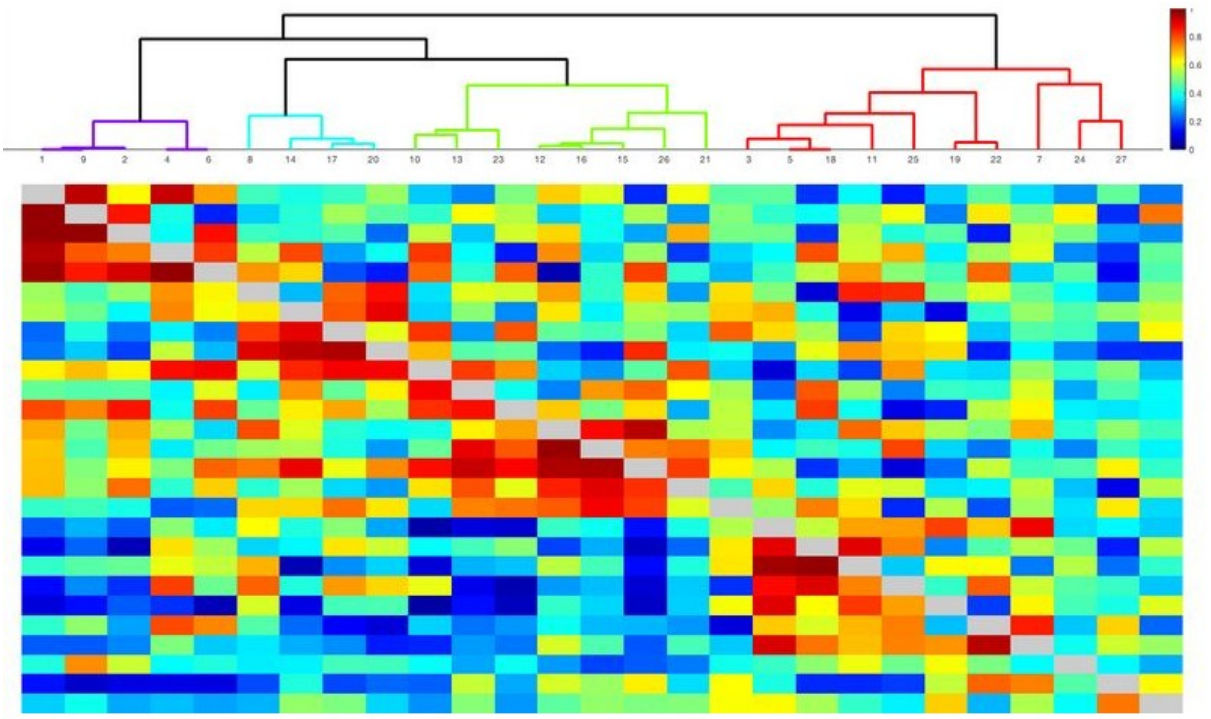

Fig. 3 Hierarchical clustering matrix, with full (below grey diagonal) and partial (above grey diagonal) correlations between-networks. The clustering yielded four groups [first group (from left to right) purple, ICs: 1, 9. 2, 4, 6; second group light blue, ICs: 8, 14, 17, 20; third group green, ICs: 10, 13, 23, 12, 16, 15, 26, 21; fourth group red, ICs: 3, 5, 18, 11, 25, 19, 22, 7, 24, 27]. IC, independent component.

3.4. Group differences in between-network connectivity

The analysis for the between-network connectivity showed a significantly increased positive coupling between IC 24 (ECN) and IC 27(SMN) in the placebo group ($p = 0.0146$, corrected for multiple comparisons across all 729 edges, Fig. 4 and Fig. 5) when compared to the nocebo group. No significant between-network connectivity could be found for the nocebo group. Specifically, IC 24 comprised the cingulate cortex, supplementary motor cortex and insular cortex areas. Additionally, activation within the amygdala, hippocampus and the brain stem was also significant. IC 27 comprised the postcentral gyrus, precuneus, cerebellum and the central operculum.

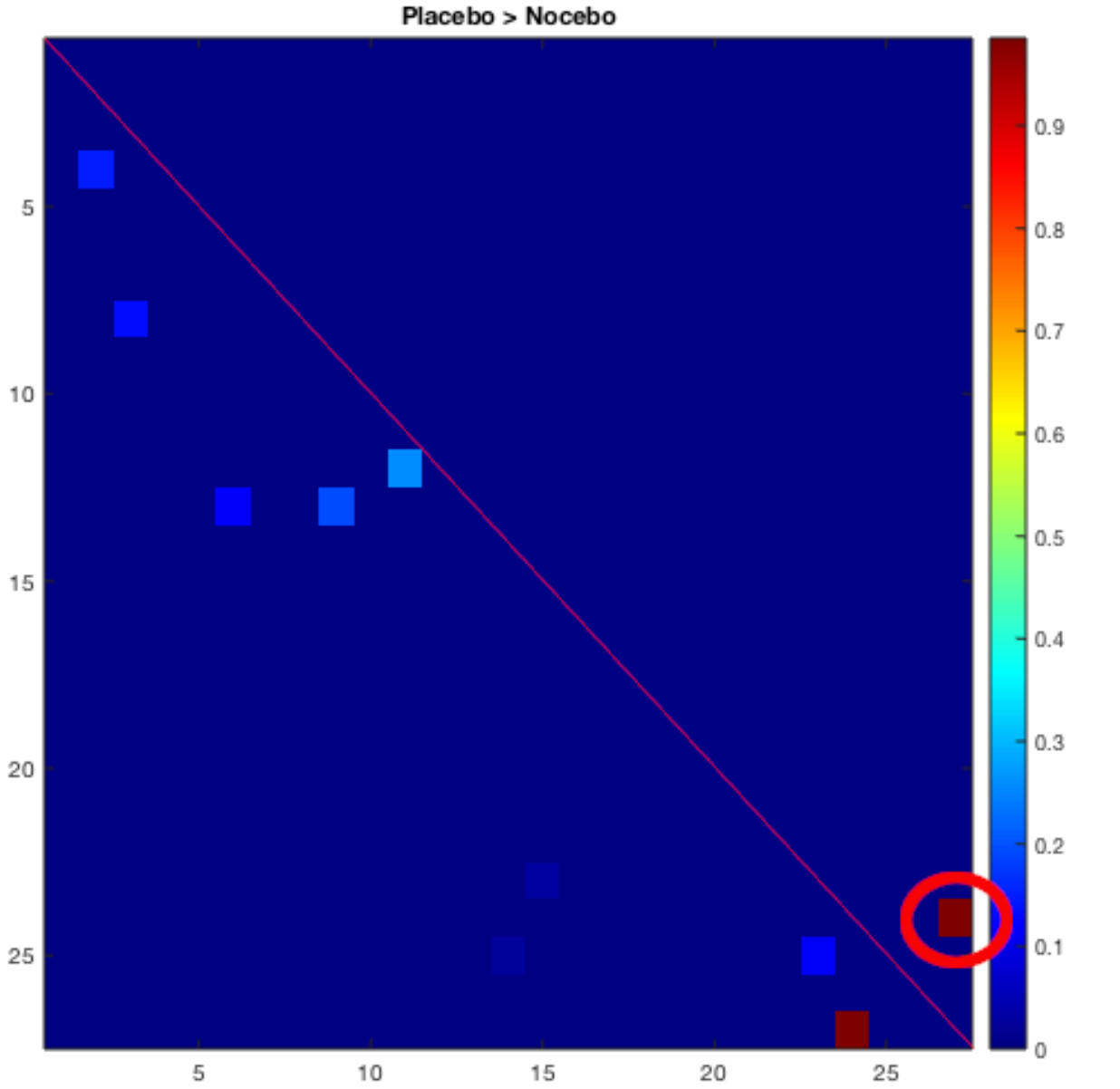

Fig. 4 Group differences for between-network connectivity. Using a general linear model design, *randomise* (using 5000 permutations) tested for between-network connectivity differences between the placebo and nocebo group. Significant finding is shown above the red diagonal and for display purpose highlighted within the red circle. Significant between-network connectivity for the nodes 27 and 24 was found in the placebo group ($p = 0.0146$). No finding above threshold was found the other comparison (Nocebo > Placebo). Bar on the right displays 1-p values.

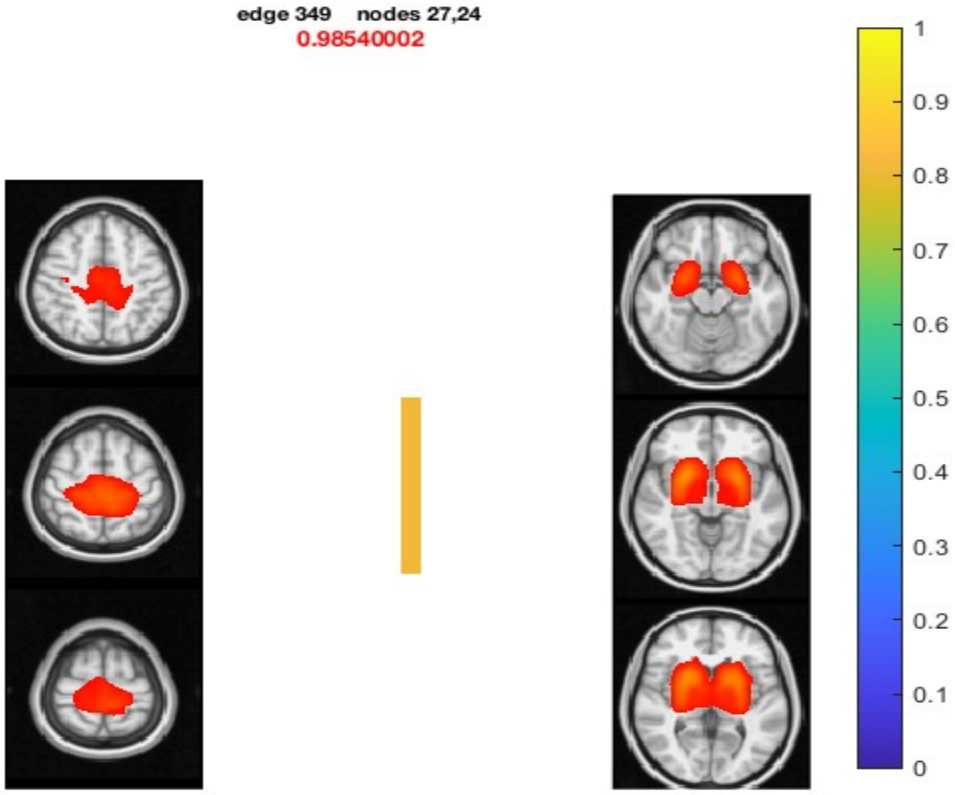

Fig 5. Closer inspection for the between-network connectivity displays a positive between-network connectivity between the nodes 27 (left) and 24 (right) at edge 349. The significance value below the nodes is presented as 1-p (p = 0.0146, corrected for multiple comparisons). The colored bar between the ICs indicates a positive correlation. IC 27 is part of the somatosensory network, showing activation around the central sulcus, which includes the postcentral gyrus, location of the primary somatosensory cortex and further activity within the precuneus, cerebellum and the central operculum. IC 24 (right) showed activation within cingulate cortex, supplementary motor cortex and insular cortex. Additionally, significant activation within the amygdala, hippocampus and the brain stem was found.

4. Discussion

This thesis assessed the influence of the placebo and nocebo effect on resting-state functional connectivity. Measuring a set of healthy participants shortly after inducing a placebo or nocebo effect through verbal suggestion and associative conditioning, the aim of this study was to investigate within-network as well as between-network connectivity differences between these groups. Results showed different activation

within the IC22, classified as resembling the DMN. A small cluster (15 voxels at 2mm³) showed significantly more connectivity in the nocebo group, labeled as belonging to the medial frontal cortex (84% probability, as indicated by *atlasquery*, reported from Oxford Cortical Structural Atlas, IC 22, Table 1). The involvement of prefrontal cortex (PFC) areas in pain modulation is repeatedly shown and it is further theorised that PFC areas are involved in a fear network (Tracey, 2010). Connectivity between the mPFC and the limbic system, mainly the basolateral and central amygdala are instrumental in the process of fear acquisition (Tovote, Fadok & Lüthi, 2015). Brown and colleagues (2014) focused on fear conditioning and found increased resting-state connectivity between different regions of the (basolateral and centromedial) amygdala, PFC areas (dorsomedial and ventromedial) and the anterior cingulate cortex (ACC). Similar findings come from Feng and colleagues (2013), where increased resting-state connectivity between ventromedial PFC and ACC was found for people that underwent fear conditioning. In opposite to the nocebo effect, Schmidt-Wilke and colleagues (2014) found decreased functional connectivity between the ACC and dorsolateral PFC in a placebo group, which would indicate a shared mechanism of the placebo and nocebo effect, influenced through different connectivity strength. Although the present results are relatively small and interpretation should be done cautiously, it further supports that expectation of higher pain intensity led to related processes in the nocebo group, as indicated by the higher within-connectivity of PFC areas. Additional support for this finding comes from the ratings of expected effectiveness that were obtained during the experimental manipulation at pre- and post-conditioning. For both groups, believed effectiveness went significantly with the direction of the suggested effect. This could reflect reappraisal of the nociceptive stimuli, indicating attentional and emotional processesing which can modulate experienced pain (Wiech, Ploner & Tracey, 2008).

Although IC22 also comprised the ACC, an assessment of potential increased connectivity between these areas is not possible. A region of interest (ROI) for the PFC, ACC and the amygdala after nocebo conditioning might be more sensitive to get decisive information of related connectivity changes in these areas. Concerning the within-network connectivity results, a positive coupling between the ICs 24 and 27 in the placebo group could be found. IC 24 comprised supplementary motor areas, insular cortex, frontal orbital cortex, superior temporal gyrus, dorsal anterior cingulate cortex and activation within the amygdala, hippocampus and the brainstem. IC 27 showed activation within the primary somatosensory cortex, superior parietal lobe, cerebellum and the lateral central operculum. Importantly, increased connectivity of the thalamus, brainstem regions, rostral and dorsal ACC and the insula might reflect placebo-induced, endogenous opioidergic activation, related to the descending pathway of pain modulation (Zunhammer et al., 2018; Wagner et al., 2019). Fox and colleagues (2005) postulate that regions that are similarly modulated by task or stimuli tend to exhibit correlated spontaneous fluctuations even in the absence of tasks or stimuli. As IC 24 and IC 27 share circuits of the descending pathway for pain modulation, this between-network connectivity could reflect a placebo effect, induced through anticipatory effects before actual pain processing.

Correlating these findings with behavioural responses from the pain ratings and the empathy for pain task could have given additional information. Especially since another master's thesis, which analysed the pain ratings and the empathy for pain task could identify a decreased pain perception and unpleasantness in the empathy for pain task from this study (Atri, 2019). This correlation could further show whether individual differences in the positive network coupling are associated with decreased individual pain intensity scores.

Overall, these findings replicate previous results relating to processes of the nocebo and placebo effect. The increased positive between-network connectivity in the placebo group indicates changes during resting-state in brain areas similar to those during pain perception, while the nocebo group showed higher prefrontal cortex activity in a network which might be related to environmental threat encoding. As the within and between-network analysis yielded results only for the placebo group, the question whether the placebo and nocebo effect have distinct or similar resting-state patterns cannot be answered here because of limited results and that several limitations need to be taken into consideration.

First, the experimental manipulation of administering an inactive pill might not be optimal to fully capture placebo and nocebo effects. In a series of studies, Jensen and colleagues could show that the placebo and nocebo effect can be induced through unconscious, subliminal stimuli (Jensen et al., 2012; Jensen et al., 2014; Jensen, Kirsch, Odmalm, Kaptchuk & Ingvar, 2015). They conclude that subcortical processing precedes higher cognitive processing. This is in line with the findings from Benedetti and colleagues (2003), who showed that conditioned immune and endocrine placebo responses still persisted after saline placebo, even after verbal information of the ineffectiveness. Therefore, conscious expectations only partly induce placebo effects. Applying dynamic functional connectivity analysis could be a potential method to reveal more information about these potentially early subcortical processes. The use of static functional connectivity and the resulting RSNs are known to be relatively stable across longer timescales (Laumann et al., 2015), but evidence suggests that spontaneous functional connectivity may vary on the order of tens of seconds. The sliding-window correlation analysis, in which functional connectivtiy is repeatedly calculated within subjects across multiple distinct temporal windows within a single resting-state session

is one popular approach (Necka, Lee, Kucyi, Cheng, Yu & Atlas, 2019). Combining both approaches, subliminal conditioning and dynamic functional connectivity might therefore provide important insight into early processes of the placebo and nocebo effect and give further insight into the dynamic processes, which already challenge the notion of a pain matrix into a dynamic pain connectome (Kucyi & Davis, 2015). Additionally, including another resting-state measurement after the experiment might also give more insight into resting-state differences between placebo and nocebo effects. From a time perspective, measuring RSNs after conditioning is a good way to minimize confounding variables, but might be more limited to cognitive evaluation of believed effectiveness opposed to longer induced effects reinforced through repeated stimuli exposure. It is also not clear if administering a pill in the control condition might have influenced the believed effectiveness. We found within-network differences by the inclusion of control sessions for the nocebo group, but no findings above threshold without the control sessions. Although not significant, the comparison of the control sessions also showed below-threshold differences within IC22 for the nocebo group ($control_{nocebo}$ vs $control_{placebo}$). Whether this comes from order effects, as believes of effectiveness could be carried over from the experimental session cannot be answered. Further, considering that already believed assumptions of treatments also influence effectiveness of the placebo and nocebo effect (Tracey, 2010), the lactose pill in the control condition might be good for the similarity of sessions, but could induce unwanted effects based on preexisting expectancies instead of order effects. Especially since the verbal information for the control group was that the medication would lead to a change in pain perception (without specified direction), this could have influenced expectancies. Also, the influence of personality factors in placebo and nocebo responsiveness can further be considered. Corsi and Colloca (2017) advise the inclusion of questionnaires

related to personality factors, as it could be shown that much variety of the responsiveness was related to personality factors.

Therefore, future studies with the inclusion of different methods are needed to further produce insight on the different mechanisms of the placebo and nocebo effect. As direct comparisons of nocebo and placebo influences on RSNs are scarce, these findings indicate that resting-state connectivity changes similar to those observable during active pain processing. But whether this reflects different mechanisms for both effects cannot be answered by these results.

5. Conclusion

To conclude, this master thesis assessed how the induction of the placebo and nocebo effect influenced resting-state functional connectivity. Imaging data from a resting-period after placebo or nocebo induction was measured. The results showed similarities of RSNs with areas involved during active placebo and nocebo processing. Specifically, the nocebo group showed higher connectivity of medial prefrontal cortex areas within the DMN, potentially indicating fear/anxiety modulation. The placebo group showed increased connectivity between-networks (IC 24 and 27) that comprised the descending pathway for pain modulation (namely the cingulate cortex, amygdala and the brain stem). This suggests that expectations of treatment influence resting-state connectivity similar to activity found during active pain processing. This further highlights the potential of resting-state connectivity analyses as a promising tool to understand and predict pain processing.

References

Amanzio, M., Benedetti, F., Porro, C. A., Palermo, S., & Cauda, F. (2011). Activation likelihood estimation meta-analysis of brain correlates of placebo analgesia in human experimental pain. *Human Brain Mapping*, n/a–n/a. doi:10.1002/hbm.21471

Andersson, J. L., Jenkinson, M., & Smith, S. (2007). Non-linear registration aka Spatial normalisation FMRIB Technial Report TR07JA2. FMRIB Analysis Group of the University of Oxford.

Atlas, L. Y., & Wager, T. D. (2014). A meta-analysis of brain mechanisms of placebo analgesia: consistent findings and unanswered questions. *In Placebo* (pp. 37-69). Springer, Berlin, Heidelberg. Doi:10.1007/978-3-662-44519-8_3

Atri, Sahand. Effects of Placebo Analgesia and Nocebo Hyperalgesia on Direct Pain and Empathy for Pain. Wien, 2019. Print.

Beckmann, C., Mackay, C., Filippini, N., & Smith, S. (2009). Group comparison of resting-state FMRI data using multi-subject ICA and dual regression. *Neuroimage*, *47*, S148. doi:10.1016/s1053-8119(09)71511-3

Benedetti, F., Pollo, A., Lopiano, L., Lanotte, M., Vighetti, S., & Rainero, I. (2003). Conscious expectation and unconscious conditioning in analgesic, motor, and hormonal placebo/nocebo responses. *Journal of Neuroscience*, *23*(10), 4315-4323. doi:10.1523/jneurosci.23-10-04315.2003

Benedetti, F., Mayberg, H. S., Wager, T. D., Stohler, C. S., & Zubieta, J. K. (2005). Neurobiological mechanisms of the placebo effect. *Journal of Neuroscience*, *25*(45), 10390-10402. doi:10.1523/jneurosci.3458-05.2005

Brown, V. M., LaBar, K. S., Haswell, C. C., Gold, A. L., McCarthy, G., & Morey, R. A. (2013). Altered Resting-State Functional Connectivity of Basolateral and

Centromedial Amygdala Complexes in Posttraumatic Stress Disorder. *Neuropsychopharmacology, 39*(2), 351–359. doi:10.1038/npp.2013.197

Colloca, L., & Grillon, C. (2014). Understanding Placebo and Nocebo Responses for Pain Management. *Current Pain and Headache Reports*, *18*(6). doi:10.1007/s11916-014-0419-2

Colloca, L., Schenk, L. A., Nathan, D. E., Robinson, O. J., & Grillon, C. (2019). When Expectancies Are Violated: A Functional Magnetic Resonance Imaging Study. *Clinical Pharmacology & Therapeutics*. doi:10.1002/cpt.1587

Colloca, L. (2017). Nocebo effects can make you feel pain. *Science*, *358*(6359), 44-44. doi:10.1126/science.aap8488

Corsi, N., & Colloca, L. (2017). Placebo and Nocebo Effects: The Advantage of Measuring Expectations and Psychological Factors. *Frontiers in Psychology, 8,* 308 doi:10.3389/fpsyg.2017.00308

Damoiseaux, J. S., Rombouts, S. A. R. B., Barkhof, F., Scheltens, P., Stam, C. J., Smith, S. M., & Beckmann, C. F. (2006). Consistent resting-state networks across healthy subjects. *Proceedings of the National Academy of Sciences*, *103*(37), 13848–13853. doi:10.1073/pnas.0601417103

De Luca, M., Beckmann, C. F., De Stefano, N., Matthews, P. M., & Smith, S. M. (2006). fMRI resting-state networks define distinct modes of long-distance interactions in the human brain. *NeuroImage, 29*(4), 1359–1367. doi:10.1016/j.neuroimage.2005.08.035

Egorova, N., Yu, R., Kaur, N., Vangel, M., Gollub, R. L., Dougherty, D. D., ... & Camprodon, J. A. (2015). Neuromodulation of conditioned placebo/nocebo in heat pain: anodal vs. cathodal transcranial direct current stimulation to the right dorsolateral prefrontal cortex. *Pain*, *156*(7), 1342. doi:10.1097/j.pain.0000000000000163

Ellerbrock, I., Wiehler, A., Arndt, M., May, A. (2015). Nocebo context modulates long-term habituation to heat pain and influences functional connectivity of the operculum. *Pain 156*(11), 2222–2233. doi:10.1097/j.pain.0000000000000297

Feng, T., Feng, P., & Chen, Z. (2013). Altered resting-state brain activity at functional MRI during automatic memory consolidation of fear conditioning*. Brain Research, 1523,* 59–67*.* doi:10.1016/j.brainres.2013.05.039

Fox, M. D., Snyder, A. Z., Vincent, J. L., Corbetta, M., Van Essen, D. C., & Raichle, M. E. (2005). The human brain is intrinsically organized into dynamic, anticorrelated functional networks. *Proceedings of the National Academy of Sciences*, *102*(27), 9673-9678. doi:10.1073/pnas.0504136102

Freeman, S., Yu, R., Egorova, N., Chen, X., Kirsch, I., Claggett, B., … Kong, J. (2015). Distinct neural representations of placebo and nocebo effects. *NeuroImage*, *112,* 197–207. doi:10.1016/j.neuroimage.2015.03.015

Greicius, M. D., Supekar, K., Menon, V., & Dougherty, R. F. (2008). Resting-State Functional Connectivity Reflects Structural Connectivity in the Default Mode Network*. Cerebral Cortex, 19*(1), 72–78*.* doi:10.1093/cercor/bhn059

Hashmi, J. A., Baria, A. T., Baliki, M. N., Huang, L., Schnitzer, T. J., & Apkarian, V. A. (2012). Brain networks predicting placebo analgesia in a clinical trial for chronic back pain*. Pain, 153*(12), 2393–2402. doi:10.1016/j.pain.2012.08.008

Jenkinson, M., Bannister, P., Brady, J. M. and Smith, S. M. (2002) Improved Optimisation for the Robust and Accurate Linear Registration and Motion Correction of Brain Images. *NeuroImage, 17*(2), 825-841. doi:10.1016/s1053-8119(02)91132-8

Jenkinson, M. (2001). Improved unwarping of EPI images using regularised B0 maps. *NeuroImage*, *6*(13), 165. doi:10.1016/s1053-8119(01)91508-3

Kong, J., Gollub, R. L., Polich, G., Kirsch, I., LaViolette, P., Vangel, M., … Kaptchuk, T. J. (2008). A Functional Magnetic Resonance Imaging Study on the Neural Mechanisms of Hyperalgesic Nocebo Effect. *Journal of Neuroscience, 28*(49), 13354–13362. doi:10.1523/jneurosci.2944-08.2008

Kong, J., Jensen, K., Loiotile, R., Cheetham, A., Wey, H.-Y., Tan, Y., … Gollub, R. L. (2013). Functional connectivity of the frontoparietal network predicts cognitive modulation of pain*. Pain, 154*(3), 459–467*.* doi:10.1016/j.pain.2012.12.004

Kong, J., Gollub, R. L., Polich, G., Kirsch, I., LaViolette, P., Vangel, M., ... & Kaptchuk, T. J. (2008). A functional magnetic resonance imaging study on the neural mechanisms of hyperalgesic nocebo effect. *Journal of Neuroscience*, *28*(49), 13354-13362. doi:10.1523/jneurosci.2944-08.2008

Kucyi, A., & Davis, K. D. (2015). The dynamic pain connectome. *Trends in Neurosciences, 38*(2), 86–95. doi:10.1016/j.tins.2014.11.006

Nickerson, L. D., Smith, S. M., Öngür, D., & Beckmann, C. F. (2017). Using dual regression to investigate network shape and amplitude in functional connectivity analyses. *Frontiers in neuroscience*, *11*, 115. doi:10.3389/fnins.2017.00115

Laumann, T. O., Gordon, E. M., Adeyemo, B., Snyder, A. Z., Joo, S. J., Chen, M. Y., ... & Schlaggar, B. L. (2015). Functional system and areal organization of a highly sampled individual human brain. *Neuron*, *87*(3), 657-670. doi:10.1016/j.neuron.2015.06.037

Lee, J., Mawla, I., Kim, J., Loggia, M. L., Ortiz, A., Jung, C., … Napadow, V. (2019). Machine learning–based prediction of clinical pain using multimodal neuroimaging and autonomic metrics. *PAIN*, *160*(3), 550–560. doi:10.1097/j.pain.0000000000001417

Legrain, V., Iannetti, G. D., Plaghki, L., & Mouraux, A. (2011). The pain matrix reloaded: a salience detection system for the body. *Progress in neurobiology*, *93*(1), 111-124. doi:10.1016/j.pneurobio.2010.10.005

Levine, J., Gordon, N., & Fields, H. (1979). The mechanism of placebo analgesia. *The Lancet*, *312*(8091), 654-657. doi:10.1097/00132586-197908000-00053

Benedetti, F. (2014). Placebo Effects: From the Neurobiological Paradigm to Translational Implications. *Neuron, 84*(3), 623–637. doi:10.1016/j.neuron.2014.10.023

Lockwood, P. L., Apps, M. A., Valton, V., Viding, E., & Roiser, J. P. (2016). Neurocomputational mechanisms of prosocial learning and links to empathy. *Proceedings of the National Academy of Sciences*, *113*(35), 9763-9768. doi:10.1073/pnas.1603198113

Jenkinson, M., Pechaud, M., & Smith, S. (2005). BET2: MR-based estimation of brain, skull and scalp surfaces. In *Eleventh annual meeting of the organization for human brain mapping* (Vol. 17, p. 167).

Jenkinson, M., & Smith, S. (2001). A global optimisation method for robust affine registration of brain images. *Medical image analysis*, *5*(2), 143-156.

Mantini, D., Perrucci, M. G., Del Gratta, C., Romani, G. L., & Corbetta, M. (2007). Electrophysiological signatures of resting-state networks in the human brain. *Proceedings of the National Academy of Sciences, 104*(32), *13170–13175.* doi:10.1073/pnas.0700668104

Melzack, R. (1990). Phantom limbs and the concept of a neuromatrix. *Trends in Neurosciences, 13*(3), 88–92. doi:10.1016/0166-2236(90)90179-e

Mouraux, A., Diukova, A., Lee, M. C., Wise, R. G., & Iannetti, G. D. (2011). A multisensory investigation of the functional significance of the "pain matrix". *Neuroimage*, *54*(3), 2237-2249. doi:10.1016/j.neuroimage.2010.09.084

Palacios, E. M., Yuh, E. L., Chang, Y.-S., Yue, J. K., Schnyer, D. M., Okonkwo, D. O., … Mukherjee, P. (2017). Resting-State Functional Connectivity Alterations Associated with Six-Month Outcomes in Mild Traumatic Brain Injury. *Journal of Neurotrauma*, *34*(8), 1546–1557. doi:10.1089/neu.2016.4752

Pollo, A., & Benedetti, F. (2013). Pain and the placebo/nocebo effect. *In Handbook of pain and palliative care* (pp. 331-346). Springer, New York, NY. Doi:10.1007/978-1-4419-1651-8_20

Pruim RHR, Mennes M, Buitelaar JK, Beckmann CF (2015a) Evaluation of ICA-AROMA and alternative strategies for motion artifact removal in resting-state fMRI. *Neuroimage 112,* 278–287. doi:10.1016/j.neuroimage.2015.02.063

Pruim RHR, Mennes M, van Rooij D, Llera A, Buitelaar JK, Beckmann CF (2015b) ICA-AROMA: A robust ICAbased strategy for removing motion artifacts from fMRI data. *Neuroimage* 112, 267–277. doi:10.1016/j.neuroimage.2015.02.064

Rief, W., Bingel, U., Schedlowski, M., & Enck, P. (2011). Mechanisms involved in placebo and nocebo responses and implications for drug trials. *Clinical Pharmacology & Therapeutics*, *90*(5), 722-726. doi:10.1038/clpt.2011.204

Rütgen, M., Seidel, E. M., Riečanský, I., & Lamm, C. (2015). Reduction of empathy for pain by placebo analgesia suggests functional equivalence of empathy and first-hand emotion experience. *Journal of Neuroscience*, *35*(23), 8938-8947. doi:10.1523/jneurosci.3936-14.2015

Schmidt-Wilcke, T., Ichesco, E., Hampson, J. P., Kairys, A., Peltier, S., Harte, S., … Harris, R. E. (2014). resting-state connectivity correlates with drug and placebo response in fibromyalgia patients. *NeuroImage: Clinical, 6,* 252–261. doi:10.1016/j.nicl.2014.09.007

Smith, S. M., Jenkinson, M., Woolrich, M. W., Beckmann, C. F., Behrens, T. E. J., Johansen-Berg, H., … Matthews, P. M. (2004). Advances in functional and structural MR image analysis and implementation as FSL. NeuroImage, 23, S208–S219. doi:10.1016/j.neuroimage.2004.07.051

Salomons, T. V., Iannetti, G. D., Liang, M., & Wood, J. N. (2016). The “pain matrix” in pain-free individuals. *JAMA neurology*, *73*(6), 755-756. doi:10.1001/jamaneurol.2016.0653

Schmidt-Wilcke, T., Ichesco, E., Hampson, J. P., Kairys, A., Peltier, S., Harte, S., … Harris, R. E. (2014). Resting-state connectivity correlates with drug and placebo response in fibromyalgia patients. *NeuroImage: Clinical, 6,* 252–261. doi:10.1016/j.nicl.2014.09.007

Smith, A. M., Lewis, B. K., Ruttimann, U. E., Ye, F. Q., Sinnwell, T. M., Yang, Y., … Frank, J. A. (1999). Investigation of Low Frequency Drift in fMRI Signal. *NeuroImage*, *9*(5), 526–533. doi:10.1006/nimg.1999.0435

Smith SM, Nichols TE (2009). Threshold-free cluster enhancement: addressing problems of smoothing, threshold dependence and localisation in cluster inference. *Neuroimage.*, *44*(1), 83-98. doi:10.1016/j.neuroimage.2008.03.061

Testa, M., & Rossettini, G. (2016). Enhance placebo, avoid nocebo: How contextual factors affect physiotherapy outcomes. *Manual Therapy*, *24*, 65–74. doi:10.1016/j.math.2016.04.006

Terkelsen, A. J., Andersen, O. K., Mølgaard, H., Hansen, J., & Jensen, T. S. (2004). Mental stress inhibits pain perception and heart rate variability but not a nociceptive withdrawal reflex. *Acta physiologica scandinavica*, *180*(4), 405-414. doi:10.1111/j.1365-201x.2004.01263.x

Tovote, P., Fadok, J. P., & Lüthi, A. (2015). Neuronal circuits for fear and anxiety. *Nature Reviews Neuroscience*, *16*(6), 317-331. doi:10.1038/nrn3945

Tracey, I., & Johns, E. (2010). The pain matrix: reloaded or reborn as we image tonic pain using arterial spin labelling. *Pain*, *148*(3), 359-360.

Tracey, I., & Mantyh, P. W. (2007). The cerebral signature for pain perception and its modulation. *Neuron*, *55*(3), 377-391. doi:10.1016/j.neuron.2007.07.012

Van de Sand, M. F., Menz, M. M., Sprenger, C., & Büchel, C. (2018). Nocebo-induced modulation of cerebral itch processing–an fMRI study. *Neuroimage*, *166*, 209-218. doi:10.1016/j.neuroimage.2017.10.056

Van den Heuvel, M. P., & Hulshoff Pol, H. E. (2010). Exploring the brain network: A review on resting-state fMRI functional connectivity. European *Neuropsychopharmacology*, *20*(8), 519–534. doi:10.1016/j.euroneuro.2010.03.008

Wager, T. D., & Atlas, L. Y. (2015). The neuroscience of placebo effects: connecting context, learning and health. *Nature Reviews Neuroscience*, *16*(7), 403-418. doi:10.1038/nrn3976

Wager, T. D., Atlas, L. Y., Lindquist, M. A., Roy, M., Woo, C. W., & Kross, E. (2013). An fMRI-based neurologic signature of physical pain. *New England Journal of Medicine*, *368*(15), 1388-1397.

Wager, T. D. (2005). Expectations and anxiety as mediators of placebo effects in pain. *Pain, 115*(3), 225–226. doi:10.1016/j.pain.2005.03.018

Wiech, K., Ploner, M., & Tracey, I. (2008). Neurocognitive aspects of pain perception. *Trends in cognitive sciences*, *12*(8), 306-313. doi:10.1016/j.tics.2008.05.005

Winkler, A. M., Ridgway, G. R., Webster, M. A., Smith, S. M., & Nichols, T. E. (2014). Permutation inference for the general linear model. *NeuroImage, 92*, 381–397. doi:10.1016/j.neuroimage.2014.01.060

Zaccara, G., Giovannelli, F., & Schmidt, D. (2015). Placebo and nocebo responses in drug trials of epilepsy. *Epilepsy & Behavior*, *43,* 128–134. doi:10.1016/j.yebeh.2014.12.004

Zhang, Y. and Brady, M. and Smith, S. (2001). Segmentation of brain MR images through a hidden Markov random field model and the expectation-maximization algorithm. *IEEE Trans Med Imag, 20*(1):45-57. doi:10.1109/42.906424

Zunhammer, M., Bingel, U., & Wager, T. D. (2018). Placebo Effects on the Neurologic Pain Signature. *JAMA Neurology, 75*(11), 1321. doi:10.1001/jamaneurol.2018.2017